Clinics in Surgery

Research Article
Published: 15 Feb, 2022

Identification of *FGFR1* Mutations in Patients with Sporadic Conotruncal Defect

Wenting Song[1,2#], Shuang Zhou[2#], Jieru Lu[1,2], Yu Wang[1,2], Qingjie Wang[2], Jian Wang[2], Zhuo Meng[2], Jiayu Peng[2], Yue Zhou[2], Sun Chen[2], Yurong Wu[2] and Kun Sun[1,2]**

[1]Department of Pediatric Cardiology, Wenzhou Medical University, Second Affiliated Hospital, China

[2]Department of Pediatric Cardiovascular, Xinhua Hospital Affiliated to Shanghai Jiaotong University School of Medicine, China

[#]These authors contributed equally to this work

Abstract

Background: Conotruncal Defects (CTDs), caused by dysplasia of the Outflow Tract (OFT), are heterogeneous congenital heart malformations. Recent research has shown that Fibroblast Growth Factor 1 (*FGFR1*) is closely related to Endothelial-to-Mesenchymal Transition (EMT), which implies that dysfunctional *FGFR1* can result in OFT malformation.

Methods: *FGFR1* variants were sequenced by targeted sequencing in a cohort of 604 CHD patients and population-matched healthy controls (n=300). To investigate the effect of mutations on the experience of the *FGFR1* protein, as well as the influence of EMT related proteins in HUVECs. We also identified expression of *FGFR1* in Carnegie stage 16 human embryos.

Results: Three rare heterozygous non-synonymous variants were identified in six CTD patients: The variant NM_001174063: c.173G>A (p.R58Q), referred to as rs200116660; the variant NM_001174063: c.320C>T (p.S107L) referred to as rs140382957; and the variant NM_001174063: c1271 G>A (p.R333H), referred to as rs183376882. There was a difference in expression of the variants. The expression levels of EMT related genes in the variants were altered. And we found that *FGFR1* was detected in the Outflow Tract (OFT) during human embryonic development.

Conclusion: Our results demonstrate that the p.R58Q, p.S107L and p.R333H variants of *FGFR1* contribute to CTD etiology by excessive suppression of EMT.

Keywords: *FGFR1*; Mutation; Outflow tract; Conotruncal defects; EMT

OPEN ACCESS

Correspondence:
Yurong Wu, Department of Pediatric Cardiovascular, Xinhua Hospital Affiliated to Shanghai Jiaotong University School of Medicine, China, E-mail: Wuyurong@xinhuamed.com.cn
Kun Sun, Department of Pediatric Cardiovascular, Xinhua Hospital Affiliated to Shanghai Jiaotong University School of Medicine, China, E-mail: sunkun@xinhuamed.com.cn

Received Date: *18 Nov 2021*
Accepted Date: *15 Jan 2022*
Published Date: *15 Feb 2022*

Citation:
Song W, Zhou S, Lu J, Wang Y, Wang Q, Wang J, et al. Identification of FGFR1 Mutations in Patients with Sporadic Conotruncal Defect. Clin Surg. 2022; 7: 3415.

Abbreviations

CHD: Congenital Heart Disease; CTDs: Conotruncal Defects; DORV: Double Outlet of Right Ventricle; EMT: Endothelial Mesenchymal Transformation; *FGFR1*: Fibroblast Growth Factor Receptor 1; FGFs: Fibroblast Growth Factors; *HMGA2*: High Mobility Group A2; IAA: Interrupted Aortic Arch; OFT: Outflow Tract;

PA/VSD: Pulmonary Atresia with Ventricular Septal Defect; PTA: Persistent Truncus Arteriosus; SA: Single Atrium; SHF: Second Heart Field; SV: Single Ventricle; TGA: Transposition of the Great Arteries; TGF-β: Transformed Growth Factor-β; TOF: Tetralogy of Fallot

Background

Congenital Heart Disease (CHD) is an abnormality of the overall structural of the heart, and is the most common disease of birth defect in humans. It is a common cause of abortion and fetal death, as well as appearing in about 1% of all live births [1]. Conotruncal Defect (CTD), the most common cyanotic CHD, is a severe deformity characterized by a disordered arrangement of the ventricles, aorta, and pulmonary artery, and consists of Double Outlet of Right Ventricle (DORV), Interrupted Aortic Arch (IAA), Pulmonary Atresia with Ventricular Septal Defect (PA/VSD), Persistent Truncus Arteriosus (PTA), Transposition of the Great Arteries (TGA) and Tetralogy of Fallot (TOF). CTDs, which commonly occur in infants and children and is a leading cause of infant death and childhood disability are estimated to affect about 1 out of 1,000 live births [2].

The factors involved in CHD include both genetic and non-genetic factors, such as hypoxia during pregnancy, infectious factors, history of teratogenic drug use, and environmental factors.

Although much research has been conducted on the genetic causes of CHD, only a small number of cases can be attributed to specific genetic factors [3]. Most of the genetic factors that predispose patients to CTD remain unknown [4-6]. The development of OFT is coordinated with two distinct cell types: Cardiac neural crest cells and Second Heart Field (SHF) progenitors [7]. They are involved in forming the polarity of the heart, which may affect valve formation and remodeling by affecting the development of the cardiac pad [8].

Fibroblast Growth Factors (FGFs) are a type of cell growth factor with extensive biological activities that play an important role in the formation of organs and tissues in early embryos. FGFs are known to play an important regulatory role in the OFT process and may be involved in heart valve formation. Studies have shown that FGF8 and FGF10 are located in the outflow tract during human embryonic development, and several mutations in FGF8 and FGF10 have been tested in patients with CTD [9]. Fibroblast Growth Factor Receptor 1 (*FGFR1*), a member of the FGFR family, is one of the four FGF receptors. *FGFR1* is a tyrosine protein kinase, a cell surface receptor that acts as a growth factor for fibroblasts and regulation of embryonic development, cell proliferation, differentiation and migration [10-12]. Deletion of *FGFR1* in mouse embryos leads to severe growth retardation and embryonic death [13,14]. At the same time, *FGFR1*, a key FGFR regulating the TGF-β (Transformed Growth Factor-β) signaling pathway, has been identified as an inhibitor of TGF-β to inhibit Endothelial Mesenchymal Transformation (EMT), and associates with some of the most common cardiovascular diseases [3,15]. Relevant studies have shown that p38-MAPK downregulates FGF-induced signaling [16-18]. Meanwhile, the p38-MAPK pathway is required for TGF-β-mediated EMT. p38-Mitogen-Activated Protein Kinase is required for TGFβ-mediated fibroblastic trans-differentiation and cell migration. *FGFR1* expression influences the epicardium at the full rate of myocyte proliferation in the embryonic chick heart [19], and *FGFR1*-mediated signaling is necessary for myocardial invasion in the quail heart [20]. EMT plays a key role in organ fibrosis and is involved in various pathological processes, such as cardiac fibrosis [21]. Relevant studies have shown that the TGF-β1/p38 signaling pathway is the main inducer of EMT, although non-TGF-β1 pathways, such as Notch signaling pathways, are also involved in the induction of EMT [22,23]. The High Mobility Group A2 (*HMGA2*), in association with the TGF-β regulator EMT, binds to the *SNAIL1* promoter and regulates transcriptional of *SNAIL1* expression [24].

FGFR1 is also required for the normal development of the cardiac outflow tract. Therefore, we hypothesized that harmful mutation in the *FGFR1* gene might participate in the molecular mechanisms of human CTD pathogenesis. We then screened for *FGFR1* variants in a CTD cohort and evaluated potentially deleterious variants. Here, we report three rare non-synonymous *FGFR1* variants in six patients with CTD. Our data show that these mutations altered the mRNA and protein expression of *FGFR1*. Functional analyses revealed that the variants of *FGFR1* may regulate EMT to promote CTD incidence. To our knowledge, this is the first report of a human CHD phenotype associated with genetic variation in *FGFR1*.

Methods

Study population

Population included 604 patients with sporadic non-syndromic CTD, diagnosed by echocardiography, surgery or cardiac catheterization at Shanghai Xin Hua Hospital. And our participants were from the Chinese Han population, ranging from 1 day to 17 years, included 397 males and 207 females (Table 1). We ruled out patients with known syndromes or chromosomal abnormalities. The control group comprised 300 healthy individuals without heart disease. informed consent for inclusion was provided by both patient and control groups, and Genomic DNA was collected from peripheral blood, using the QIAamp DNA Blood Mini Kit (QIAGEN, Germany), according to the manufacturer's instructions and stored at -80°C until further analysis.

Targeted sequencing and variant analysis

Targeted sequencing of *FGFR1* variants was sequenced by Illumina HiSeq 2000 platform (GenBank accession number NM_001174063). Candidate mutations were tested by Sanger sequencing, and the primers designed to amplify the coding regions containing candidate variants using Primer Premier 5 in Additional file 1: Table S1. To predict the effects of nonsynonymous variants in advance, we used several different bioinformatics criteria: Mutation Taster (http://mutationtaster.org/, SIFT (http://sift.jcvi.org/ www/SIFT_enst_submit.html) and Polyphen-2 (http://genetics.bwh.havard.edu/pph2/). It was agreed that amino acid substitutions were predicted to be harmful when the score was ≤ 0.05 in SIFT or ≥ 0.85 in Polyphen-2. At the same time, we defined a Minor Allele Frequency (MAF) <0.5% as rare [25]. All candidate *FGFR1* variants were confirmed by Sanger sequencing. The candidate gene variants were determined by their absence in Genome Aggregation Database (gnomAD) (http://gnomad.broadinstitute.org/) and the Exome Aggregation Consortium (ExAC) database (http://exac.broadinstitute.org/).

Multiple *FGFR1* protein sequence alignment

We downloaded *FGFR1* protein sequences of *Homo sapiens* (human), *Mus musculus* (house mouse), *Gallus Gallus* (chicken), *Pongo abelii* (Ponab), and *Rattus norvegicus* (Rat) from NCBI (https://www.ncbi.nlm.nih.gov/protein/) and then compared them with ClustalX software to analyze the conservation of *FGFR1* sequences.

Plasmid construction and site-directed mutagenesis

The plasmid of *FGFR1* cDNA was purchased from GenoMeditech. Variant primers were designed to amplify human *FGFR1* cDNA according to the protocol of Quick Change Site-Directed Mutagenesis

Table S1: Primer pairs used to amplify the coding regions contain candidate variants.

Candidate variant	Primer orientation	Primer sequence	Product size (bp)
c.173G>A	F	5'- ACTTTGCCTCTTTCTTCCTTTGA-3'	518
	R	5'- ATTGACGGAGAAGTAGGTGGTGT-3'	
c.320C>T	F	5'- ACTTTGCCTCTTTCTTCCTTTGA-3'	518
	R	5'- ATTGACGGAGAAGTAGGTGGTGT-3'	
c.1271G>A	F	5'- CACCCTGTTCGCACTGACTC-3'	505
	R	5'- TGCTATTGGCTGCACATTCT-3'	

Kit (Stratagene, USA), and mutated *FGFR1* cDNAs were cloned into pCMV6 vectors.

Cell cultures and transfection

Human Umbilical Vein Endothelial Cells (HUVECs) were cultured in DMEM with 10% fetal bovine serum (MP Biomedicals, USA) and 1% penicillin-streptomycin (Gibco, USA). The HUVECs were transfected with 1 μg of pGPU6-GFP-neo vector (Genepharma, China) and wild-type and variant plasmid DNA using FuGene HD (Promega, USA) according to the manufacturer's protocol after seeding for 24 h. Many studies have illustrated that there is a large amount of TGF-β1 in fetal bovine serum, enough to induce partial EMT [26]. Moreover, spontaneous EMT occurred in HUVECs during low confluence. In order to induce EMT successfully, cells were cultured in serum-free medium for 24 h, and about 70% of the fused cells were treated with TGF-β1 (Peprotech, 96-100-21-2) at a final concentration of 10 ng/ml. Note that culture medium containing TGF-β1 need to be replaced every other day.

Quantitative RT-PCR

We first transfected the plasmids into HUVECs in 12-well plates. Cells were harvested 36 h after the transfection. Next, total RNA was extracted with TRIzol reagent (Invitrogen, USA), and cDNA was reversely transcribed with Prime Script RT Master Mix (Takara, Japan). Quantitative RT-PCR used SYBR Premix Ex Taq (Takara, Japan) on an Applied Biosystems 7500 system (Applied Biosystems, USA). Relative expression levels were determined using the $2^{-\Delta\Delta C}$ [t] method [27] and Glyceraldehyde-3-Phosphate Dehydrogenase (*GAPDH*, human) was used as an internal control. Primer sequences of the *GAPDH*, *FGFR1*, *TGF-βR1*, and *SNAIL1* genes are shown in (Table 3).

Western blot

We transfected with 1 μg of wild-type and mutant plasmid DNA into HUVECs, and the cells were harvested 48 h after transfection. RIPA lysis buffer (Beyotime, China) containing PMSF (1:100) was used to lysate the cells. The proteins were transferred onto nitrocellulose membranes (Millipore, USA) using 10% SDS-PAGE, and then incubated with rabbit *FGFR1* antibody (1:1000, ABSci, USA), rabbit *HMGA2* antibody (1:1000, AVIVA, USA), and rabbit *GAPDH* antibody (1:5,000) at 4°C overnight. The membranes were then incubated with a horseradish peroxidase labeled anti-rabbit secondary antibody (1:5,000). Immobilon Western Chemiluminescent HRP Substrate (Millipore, Billerica, MA, USA) was used for chemiluminescent immunodetection using the Image J program (BioRad, Philadelphia, PA, USA).

Tissue collection and microarray experiment

Human embryo heart samples of CS10-16 were obtained after termination of pregnancy at Shanghai Xinhua Hospital. We used Tissue Lyser II (Qiagen) and RN easy Min Elute Cleanup Kit (Qiagen) to extract total RNA. Gene expression levels at different developmental stages were detected by transcriptome microarray analysis. Affymetrix Transcriptome Analysis Console (TAC) software was used to normalize the original data, and the normalized signal values were calculated by log2 transformation.

Immunofluorescence assay

The embryos were fixed in 4% paraformaldehyde solution for 16 h to 24 h, embedded in paraffin, and then sectioned at a thickness of 5 μm, paraffin sections were permeabilized using 0.3% Triton X-100 for 10 min, and blocked with 5% BSA at 25°C for 1 h. Following, paraffin sections were incubated with mouse anti-human *FGFR1* (1:50; CST) antibody and anti-rabbit Islet1 (1:50; CST) at 4°C overnight, followed by incubation with secondary anti-mouse-Alexa Flour 488 (1:100; invitrigen) and Cy3-conjugated goat anti-rabbit (1:100; Jackson, USA) for at least 2 h at 37°C. Nuclei were then tinted with 4,6-Diamidino-2-Phenylindole (DAPI; Vector Laboratories, USA) for 7 min at room temperature. Olympus BX43 microscope (Olympus, Shinjukuku, Tokyo, Japan) was used for image acquisition and analysis.

Statistical analysis

Each molecular experiment has three separate biological replicates. Data are expressed as mean ± Standard Deviation (SD). The independent-samples t-test was used to determine statistical significance of unpaired samples. Moreover, bilateral statistical tests were considered to have significant with a level of $p<0.05$. In this study, SPSS 22.0 (SPSS Inc. Chicago, IL, USA) was used for all statistical analysis.

Results

The variants of *FGFR1* identified in patients with CTD

We identified *FGFR1* variants by targeted sequencing in 604 patients with CTD and identified 3 variants of *FGFR1* in 6 patients whose diagnoses included TOF, DORV, SA, and SV (Table 2). Three heterozygous missense variants in *FGFR1* were identified in 6 unrelated patients among 604 patients with CTD. None of the 300 controls subjects in our cohort: p.R58Q in SA/SV, p.S107L in TOF and DORV, and p.R333H in TOF (Figure 1b, 1d, 1f). However, all of these variants resulted in amino acid substitutions without exception and were predicted to be destructive by SIFT, Polyphen-2, or Mutation Taster (Table 1).

Alignment of multiple *FGFR1* protein sequences and display of the structure of human *FGFR1* protein

All variation sites above were highly conserved as shown by multiple *FGFR1* protein alignments (Figure 2a), indicating that these variants are very important and might lead to gene function alterations in *FGFR1*. Human *FGFR1* spans 289,552 bp, and has been mapped to chromosome 8p11.23, which is composed of 24 exons and

Table 1: Clinical information and variant characteristics of FGFR1 in patients with CHD.

Patient	Gender	Age	Cardiac phenotype	Gene	Location in gene	Function	Nucleotide change	Amino acid change	dbSNP ID	SIFT	Mutation taster	PolyPhen-2	ExAC/ gnomAD
1	M	8 months	SA/SV	FGFR1	exon3	Missense	173G>A	R58Q	rs200116660	0.01	0.844078	0.752	0.000017/0.000218
2	F	7 months	TOF	FGFR1	exon3	Missense	320C>T	S107L	rs140382957	0.07	0.985398	0.292	0.002526/0.018
3	M	1 months	DORV	FGFR1	exon3	Missense	320C>T	S107L	rs140382957	0.07	0.985398	0.292	0.002526/0.018
4	M	6 months	DORV	FGFR1	exon3	Missense	320C>T	S107L	rs140382957	0.07	0.985398	0.292	0.002526/0.018
5	M	1 year	TOF	FGFR1	exon9	Missense	1271G>A	R333H	rs183376882	0.06	0.999984	0.01	0.000058/0.0001669
6	M	8 months	TOF	FGFR1	exon9	Missense	1271G>A	R333H	rs183376882	0.06	0.999984	0.01	0.000058/0.0001669

M: Male; F: Female; SA: Single Atrium; SV: Single Ventricle; TOF: Tetralogy of Fallot; DORV: Double Outlet Right Ventricle

Table 2: Cardiac diagnoses for study population of patients with CHDs.

Diagnoses	Number	Gender/number	Age
TOF	231	F81M150	1 month - 13 years
DORV	100	F34M66	1 month - 17 years
PA/VSD	98	F37M61	3 months - 12 years
TGA	94	F22M72	1 day - 16 years
SA/SV	46	F19M27	1 month - 13 years
IAA	13	F7M6	7 days - 1 year
PA/IVS	12	F2M10	2 days - 4 years
PTA	10	F5M5	3 days - 2 years
Total	604	F207M397	1 day - 17 years

M: Male; F: Female; TOF: Tetralogy of Fallot; DORV: Double Outlet Right Ventricle: PA/VSD: Pulmonary Atresia with Ventricular Septal Defect; TGA: Transposition of the Great Arteries; SA: Single Atrium; SV: Single Ventricle; IAA: Interruption of Aortic Arch; PA/IVS: Pulmonary Atresia with Intact Ventricular Septum; PTA: Persistent Truncus Arteriosus

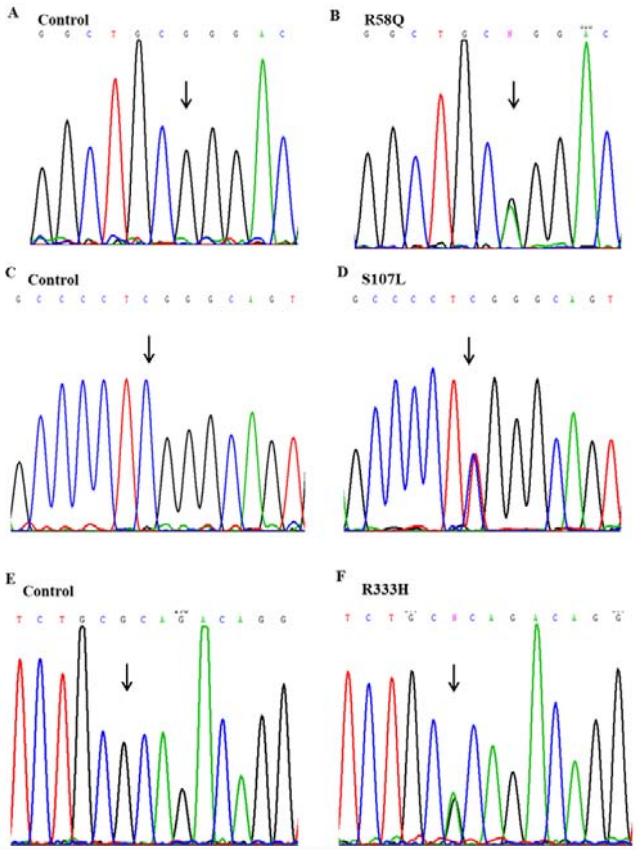

Figure 1: Sequence chromatograms of FGFR1. A, C) and E**)** N normal controls. B, D and F) Heterozygous variants. Arrow show heterozygous nucleotide changes.

23 introns (Figure 2b) (http://www.uniprot.org/).

Detection of *FGFR1* variant expression

To investigate whether the transfection was successfully conducted, we used GFP to confirm that the transfection system was working by fluorescence detection. To investigate whether the transfection was successfully conducted and whether the expression of *FGFR1* was altered, we performed quantitative RT-PCR and western blotting in the non-TGF-β-induced and TGF-β-induced groups. Quantitative RT-PCR analysis revealed that the mRNA

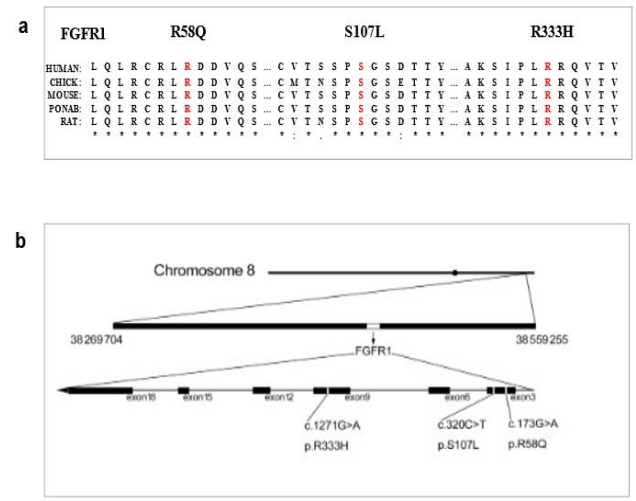

Figure 2: Conservation and distribution of *FGFR1* variants. A) Alignments of FGFR1 protein among different species. B**)** Schematic of the FGFR1 location of variants identified in this study.

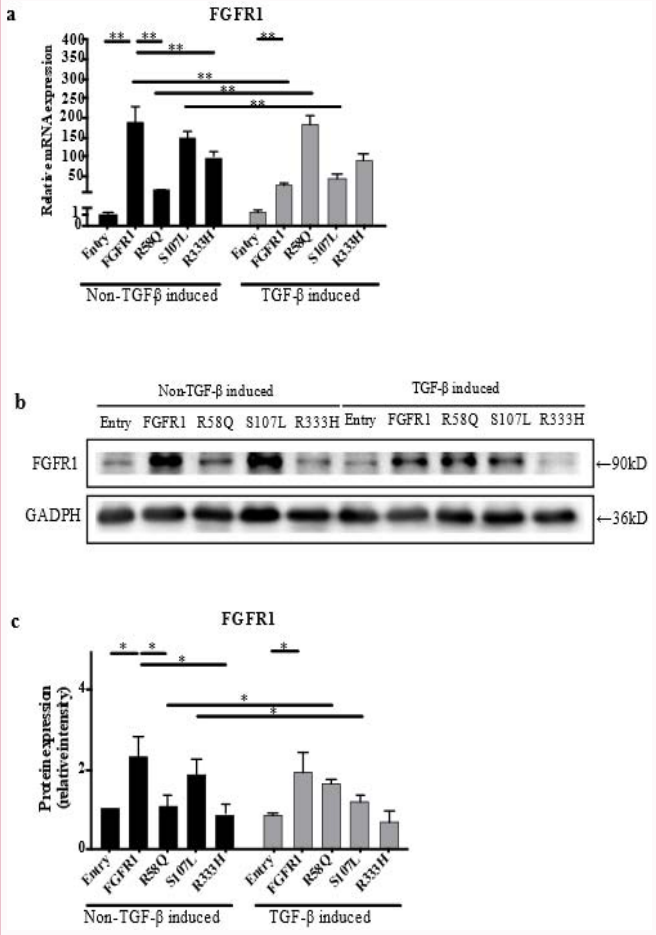

Figure 3: The expression of wild-type and mutated *FGFR1*. mRNA and protein expression level of *FGFR1* in non-TGF-β-induced and TGF-β-induced group. A) Relative mRNA expression of *FGFR1* (n=3). GADPH was used as an internal control. B, C) Western blot analysis of *FGFR1* (n=3). GADPH was used as an internal control. *P<0.05, **P<0.01; data represented here are obtained from three biological replicates.

expression levels of the p.R58Q and p.R333H variants of *FGFR1* (Figure 3a) were much lower than those of the wild-type plasmid

Table 3: Sequences of the primers used for real-time quantitative PCR.

Gene	Forward (5′→3′)	Reverse (5′→3′)
GAPDH	AATCCCATCACCATCTTCC	GAGTCCTTCCACGATACCAA
FGFR1	CTTCTCCGTCAATGTTTCAG	TCCACAATGCAGGTGTAGTT
TGFβR1	TTTCTGCCACCTCTGTAC	TCTTTATTGTCTGCTGCTAT
Snail1	TTACCTTCCAGCAGCCCTAC	AGCCTTTCCCACTGTCCTC
HMGA2	AGCAGCAAGAACCAACCG	TCCCAGGCAAGGCAACAT

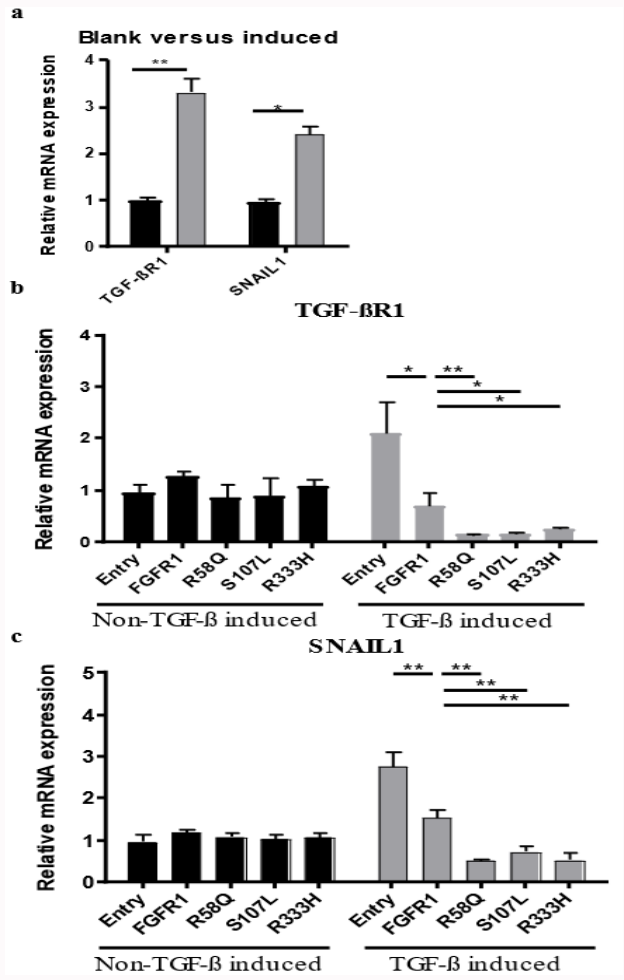

Figure 4: Functional analysis of wild-type and mutated *FGFR1* of TGF-βR. A) Relative mRNA expression in HUVECs with TGF-β-induced (n=3). B) Relative mRNA expression of TGF-βR1 (n=3). C) Relative mRNA expression of *SNAIL1* (n=3). GADPH was used as an internal control. *P<0.05, **P<0.01; data represented here are obtained from three biological replicates.

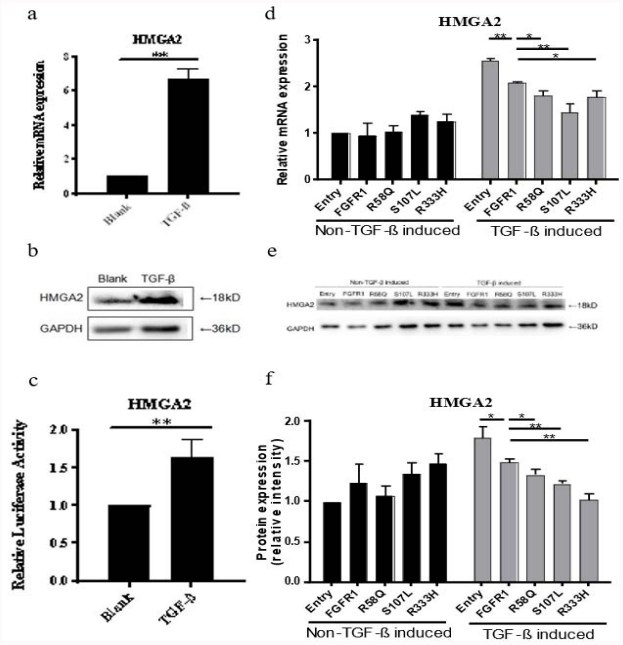

Figure 5: Mutated *FGFR1* inhibit EMT. mRNA and protein expression level of *HMGA2* of HUVECs in non-TGF-ß-induced and TGF-β-induced group. A) Relative mRNA expression of *HMGA2* of HUVECs and TGF-β-induced HUVECs (n=3). B, C) Western blot analysis of *HMGA2* of HUVECs and TGF-β-induced HUVECs (n=3). D) Relative mRNA expression of *HMGA2* (n=3). E, F) Western blot analysis of HMGA2 (n=3). GADPH was used as an internal control. *P<0.05, **P<0.01; data represented here are obtained from three biological replicates.

in the non-TGF-β-induced group. Induced by TGF-β, the mRNA expression level of *FGFR1* and the p.S107L was attenuated (Figure 3a), whereas the expression of p.R58Q was elevated. Through western blotting, we found that the protein expression of the p.R58Q and p.R333H variants (Figure 3b, 3c) was lower than that of the wild-type *FGFR1* in the non-TGF-β-induced group. Induced by TGF-β, the protein expression of p.S107L was attenuated, whereas p.R58Q was elevated (Figure 3c).

Functional analysis of *FGFR1* variant proteins

To detect the relative mRNA expression levels of EMT in HUVECs, quantitative RT-PCR was performed. Compared with HUVECs without TGF-β induction, mRNA expression levels of *FGFR1*, TGF-βR1, and *SNAIL1* were elevated with the induction of TGF-β (Figure 4a).

The mRNA expression of TGF-βR1 was increased in the blank vector and decreased in the wild type. As for the variants, quantitative RT-PCR revealed that the mRNA expression level of TGF-βR1 and *SNAIL1*, there was no difference in the expression of TGF-βR1 and *SNAIL1* between WT and mutants in untreated conditions but a significant decrease in expression when induced with TGFβ (Figure 4b, 4c).

To detect the mRNA expression level of *HMGA2* in HUVECs, quantitative RT-PCR was performed. With the induction of TGF-β, the mRNA expression level of *HMGA2* (Figure 5a) was much higher than that without TGF-β. Western blot analysis showed that the protein expression of *HMGA2* in HUVECs (Figure 5b, 5c) induced by TGF-β was greater than that without induction. The above data show that the EMT model is successful.

To examine the effect of mutated FGFR in the EMT process induced by TGF-β, quantitative RT-PCR analysis indicated that the mRNA expression level of *HMGA2* in the wild-type plasmid was lower than that of the blank vector and that the mRNA expression level of *HMGA2* in the variants (Figure 5d) was lower than that of the wild-

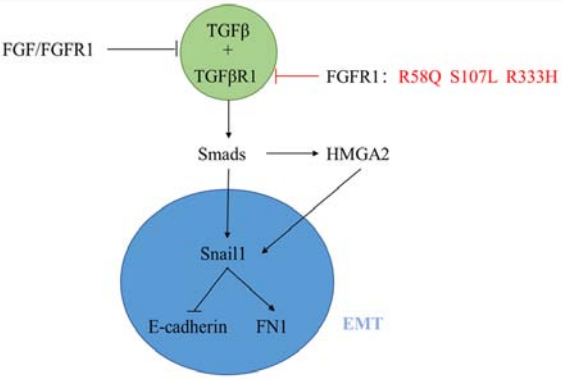

Figure 6: The diagram of the regulation *FGFR1* variants involved in CTD pathogenesis by inhibit EMT. Variants have a stronger inhibitory effect on TGF-βR1, which is suspected to be a relevant cause of conotruncal defects associated with valvular dysplasia in early outflow tracts.

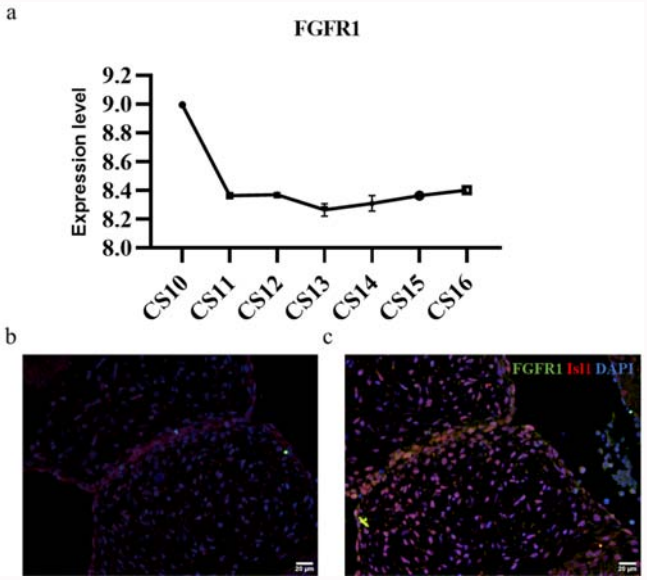

Figure 7: Dynamic expression of *FGFR1* in human embryonic cardiac tissue. A) Expression level of *FGFR1* in the human embryonic heart, B, C). Immunofluorescence assay of *FGFR1* (Green) in human embryos at Carnegie stge16.

type plasmid. Western blotting showed that the protein expression of *HMGA2* in the wild-type plasmid was less than that of the blank vector, and protein expression of *HMGA2* in the variant (Figure 5e, 5f) was much lower than that of wild-type *FGFR1*, indicating that *FGFR1* may play a role in the development of the OFT. Variants have a stronger inhibitory effect on EMT.

We also present an illustration summarizing our results and claims (Figure 6). Variants have a stronger inhibitory effect on EMT, which is suspected to be a relevant cause of conotruncal defects associated with valvular dysplasia in early outflow tracts.

Expression level of *FGFR1* in the human embryonic

FGFR1 in the human embryo has not been identified. Therefore, human embryonic hearts from CS10 to CS16 were collected and used the human transcriptome array 2.0. To analyze gene expression analysis the expression level of *FGFR1* were expressed by the mean of the sample expression levels. Our data showed that *FGFR1* were expressed at all of these development stages (Figure 7a). We then took immunohistochemistry for *FGFR1* in CS16 of human embryos. Our results showed that *FGFR1* was expressed in the OFT (Figure 7b, 7c), further supporting the role of *FGFR1* in the development of the OFT.

Discussion

Using targeted sequencing, our study showed three rare heterozygous variants of *FGFR1* in 6 out of 604 patients with sporadic CTDs including p.R58Q, p.S107L, and p.R333H, after multiple sequence alignment, First, because all of these were highly conserved, we judge that these variants might have important biological functions. These variants can be seen in Ensemble (http://ensemblgenomes.org/). However, their functions have not been studied previously. According to SIFT, Mutation Taster, or Polyphen-2, all variants were predicted to be damaging. Moreover, p.R58Q, p.S107L, p.R333H showed altered mRNA transcription and protein translation compared to wild-type *FGFR1*.

The FGF family plays an important role in maintaining the vascular endothelial cell state. Disruption of the FGF signaling pathway in endothelial cells leads to a decrease in let-7 miRNA levels, which in turn increases the activation of the TGF-β signaling pathway and promotes EMT [28]. Previous studies have reported that *FGFR1* inhibits endothelial mesenchymal transformation by inhibiting TGF-β in HUVECs [15]. *FGFR1* phosphorylation is a requirement for cardiomyocyte differentiation in murine embryonic stem cells [29], providing strong evidence that *FGFR1* is important for human cardiac morphogenesis and the underlying etiology of CTDs. *HMGA2* induces EMT by binding to the *SNAIL1* promoter and act as a transcriptional regulator of *SNAIL1* expression [24].

Endothelial mesenchymal transformation is an important physiological process in heart development especially in the OFT. We tested the response of *FGFR1* variants to TGF-βR1 in HUVECs and the changes in EMT-related indicators such as SNAILl and *HMGA2*. Furthermore, we tested the mRNA and protein expression of *HMGA2* induced by TGF-β to explore whether variants of *FGFR1* affect EMT.

In our study, higher mRNA and protein expression levels were observed in the wild-type group, than in the blank vector showed successful plasmid transfection. Meanwhile, with TGF-β induction, the mRNA expression of *SNAIL1*, TGF-βR1, and *HMGA2* was higher after induction, indicating that the TGF-β-induced model was successfully established. The significance of the TGF-β-induced model was to amplify changes in the inhibitory effect of *FGFR1* mutations on EMT. The expression of all three genes decreased with the addition of TGFβ.

As for variants, compared with the wild-type group, the mRNA expression of TGF-βR1 and *SNAIL1* was reduced in groups with TGF-β induction, while, the mRNA expression of *HMGA2* was lower upon TGF-β induction. This is consistent with the decreased protein expression observed in the *FGFR1* mutations. *HMGA2* cooperates with the TGFβ/Smad signaling pathway during the regulation of *SNAIL1* expression. *SNAIL1* acts as a major effector downstream of *HMGA2* to induce EMT [24,28]. TGF-β induces EMT in cells, by binding with TGF-βRI, activates the relevant Smad pathway, and promotes the expression of *HMGA2* protein. *HMGA2* protein acts as a transcriptional regulator and promotes the transcription of SNIAL1. *SNAIL1* promotes the transcription of FN1 associated with mesenchymal cell markers, suggesting that the occurrence of EMT, such as endocardial cells, is converted to the endocardial pad. At the same time, *HMGA2* can also promote the transcription of FN1 to

accelerate the occurrence of EMT. The TGFβ-BMP signaling axis can affect EMT by activating Smads and participating in OFT formation. Normal *FGFR1* can inhibit the occurrence of EMT by downregulating TGF-βRI, thereby affecting OFT formation.

FGFR1 involves the separation of the outflow tract, the location of the heart in the chest, the development of the pulmonary vascular system, and proliferation and maturation of the ventricular myocardium [30-33]. Previous studied have shown that dysfunction of *FGFR1* leading to heart defects has been verified in animals, with alignment defects (TGA and DORV). Effects on CNC after loss of FGF signaling in the SHF play a role in the OFT phenotypes obtained in our mesodermal FGFR and Spry2 gain-of-function mutants. Their data demonstrated the primacy of FGF signaling in the SHF mesoderm for subsequent OFT morphogenesis [34].

Of course, there were some limitations to our study. The lack of parental samples limited our ability to study the genetic background of these mutations and affected our determination of their origin. Nevertheless, this study provides the first genetic evidence that malfunctioning *FGFR1* was associated with CTDs in a large population. *FGFR1* mutations can affect valve formation by regulating the EMT process, which may be one of the mechanisms leading to CHD. However, the detailed regulation of *FGFR1* and TGF-β needs to be further studied.

Conclusion

We found that variants of *FGFR1* are associated with the occurrence of CTDs, and explored the influence of *FGFR1* mutations on EMT. Our results contribute to a better understanding of the mechanisms of CTD etiology.

Ethics Approval and Consent to Participate

All assessments were approved by the Medical Ethics Committee of Xinhua Hospital and Shanghai Children's Medical Center (XHEC-C-2019-083). All methods were carried out in accordance with the approved guidelines and regulations. Fully written informed consent was obtained from all participants or their legal guardians.

Acknowledgement

We are grateful to all participants for their contributions to this work. Thanks to the research teams of Wenzhou Medical University Second Affiliated Hospital and Xinhua Hospital affiliated to Shanghai Jiao Tong University School of Medicine for their work.

Funding

Our work was supported by the National Key R&D Program of China (No. 2018YFC1002400), and the National Natural Science Foundation of China (Grant numbers: 81720108003, 8180028).

References

1. Hoffman JI, S Kaplan, Liberthson RR. Prevalence of congenital heart disease. Am Heart J. 2004;147(3):425-39.
2. O'Malley CD, Shaw GM, Wasserman CR, Lammer EJ. Epidemiologic characteristics of conotruncal heart defects in California, 1987-1988. Teratology. 1996;53(6):374-7.
3. Moreau JLM, Kesteven S, Martin EMMA, Lau KS, Yam MX, O'Reilly VC, et al. Gene-environment interaction impacts on heart development and embryo survival. Development. 2019;146(4);dev172957.
4. Xu Y, Fang S, Zhang E, Pu T, Cao R, Fu Q. A 3 base pair deletion in TBX1 leads to reduced protein expression and transcriptional activity. Sci Rep. 2017;7:44165.
5. Lindsay EA. Chromosomal microdeletions: Dissecting del22q11 syndrome. Nat Rev Genet. 2001;2(11):858-68.
6. Robin NH, Shprintzen RJ. Defining the clinical spectrum of deletion 22q11.2. J Pediatr. 2005;147(1):90-6.
7. High FA, Jain R, Stoller JZ, Antonucci NB, Lu MM, Loomes KM, et al. Murine Jagged1/Notch signaling in the second heart field orchestrates Fgf8 expression and tissue-tissue interactions during outflow tract development. J Clin Invest. 2009;119(7):1986-96.
8. Armstrong EJ, Bischoff J. Heart valve development: Endothelial cell signaling and differentiation. Circ Res. 2004;95(5):459-70.
9. Zhou S, Wang Q, Meng Z, Peng J, Zhou Y, Song W, et al. Mutations in Fibroblast Growth Factor (FGF8) and FGF10 identified in patients with conotruncal defects. J Transl Med. 2020;18(1):283.
10. Powers CJ, McLeskey SW, Wellstein A. Fibroblast growth factors, their receptors and signaling. Endocr Relat Cancer. 2000;7(3):165-97.
11. Presta M, Dell'Era P, Mitola S, Moroni E, Ronca R, Rusnati M. Fibroblast growth factor/fibroblast growth factor receptor system in angiogenesis. Cytokine Growth Factor Rev. 2005;16(2):159-78.
12. Chen GJ, Forough R. Fibroblast growth factors, fibroblast growth factor receptors, diseases, and drugs. Recent Pat Cardiovasc Drug Discov. 2006;1(2):211-24.
13. Deng CX, Wynshaw-Boris A, Shen MM, Daugherty C, Ornitz DM, Leder P. Murine FGFR-1 is required for early postimplantation growth and axial organization. Genes Dev. 1994;8(24):3045-57.
14. Oladipupo SS, Smith C, Santeford A, Park C, Sene A, Wiley LA, et al. Endothelial cell FGF signaling is required for injury response but not for vascular homeostasis. Proc Natl Acad Sci U S A. 2014;111(37):13379-84.
15. Chen PY, Qin L, Tellides G, Simons M. Fibroblast growth factor receptor 1 is a key inhibitor of TGFbeta signaling in the endothelium. Sci Signal. 2014;7(344):ra90.
16. Zakrzewska M, Opalinski L, Haugsten EM, Otlewski J, Wiedlocha A. Crosstalk between p38 and Erk 1/2 in downregulation of FGF1-induced signaling. Int J Mol Sci. 2019;20(8):1826.
17. Sørensen V, Zhen Y, Zakrzewska M, Haugsten EM, Wälchli S, Nilsen T, et al. Phosphorylation of Fibroblast Growth Factor (FGF) receptor 1 at Ser777 by p38 mitogen-activated protein kinase regulates translocation of exogenous FGF1 to the cytosol and nucleus. Mol Cell Biol. 2008;28(12):4129-41.
18. Bakin AV, Rinehart C, Tomlinson AK, Arteaga CL. p38 mitogen-activated protein kinase is required for TGFbeta-mediated fibroblastic transdifferentiation and cell migration. J Cell Sci. 2002;115(Pt 15):3193-206.
19. Pennisi DJ, Ballard VLT, Mikawa T. Epicardium is required for the full rate of myocyte proliferation and levels of expression of myocyte mitogenic factors FGF2 and its receptor, FGFR-1, but not for transmural myocardial patterning in the embryonic chick heart. Dev Dyn. 2003;228(2):161-72.
20. Pennisi DJ, Mikawa T. FGFR-1 is required by epicardium-derived cells for myocardial invasion and correct coronary vascular lineage differentiation. Dev Biol. 2009;328(1):148-59.
21. Zeisberg EM, Tarnavski O, Zeisberg M, Dorfman AL, McMullen JR, Gustafsson E, et al. Endothelial-to-mesenchymal transition contributes to cardiac fibrosis. Nat Med. 2007;13(8):952-61.
22. Kitao A, Sato Y, Sawada-Kitamura S, Harada K, Sasaki M, Morikawa H, et al. Endothelial to mesenchymal transition *via* transforming growth factor-beta1/Smad activation is associated with portal venous stenosis in idiopathic portal hypertension. Am J Pathol. 2009;175(2):616-26.

23. Dejana E, Hirschi KK, Simons M. The molecular basis of endothelial cell plasticity. Nat Commun. 2017;8:14361.

24. Thuault S, Tan EJ, Peinado H, Cano A, Heldin CH, Moustakas A. HMGA2 and Smads co-regulate SNAIL1 expression during induction of epithelial-to-mesenchymal transition. J Biol Chem. 2008;283(48):33437-46.

25. Manolio TA, Collins FS, Cox NJ, Goldstein DB, Hindorff LA, Hunter DJ, et al. Finding the missing heritability of complex diseases. Nature. 2009;461(7265):747-53.

26. Zhang J, Tian XJ, Zhang H, Teng Y, Li R, Fan Bai F, et al. TGF-beta-induced epithelial-to-mesenchymal transition proceeds through stepwise activation of multiple feedback loops. Sci Signal. 2014;7(345):ra91.

27. Livak KJ, Schmittgen TD. Analysis of relative gene expression data using real-time quantitative PCR and the 2(-Delta Delta C(T)) Method. Methods. 2001;25(4):402-8.

28. Chen PY, Qin L, Barnes C, Charisse K, Yi T, Zhang X, et al. FGF regulates TGF-beta signaling and endothelial-to-mesenchymal transition *via* control of let-7 miRNA expression. Cell Rep. 2012;2(6):1684-96.

29. Ronca R, Gualandi L, Crescini E, Calza S, Presta M, Dell'Era P. Fibroblast growth factor receptor-1 phosphorylation requirement for cardiomyocyte differentiation in murine embryonic stem cells. J Cell Mol Med. 2009;13(8A):1489-98.

30. Beiman M, Shilo BZ, Volk T. Heartless, a *Drosophila* FGF receptor homolog, is essential for cell migration and establishment of several mesodermal lineages. Genes Dev. 1996;10(23):2993-3002.

31. Partanen J, Schwartz L, Rossant J. Opposite phenotypes of hypomorphic and Y766 phosphorylation site mutations reveal a function for Fgfr1 in anteroposterior patterning of mouse embryos. Genes Dev, 1998;12(15):2332-44.

32. Abu-Issa R, Smyth G, Smoak I, Yamamura KI, Meyers EN. Fgf8 is required for pharyngeal arch and cardiovascular development in the mouse. Development. 2002;129(19):4613-25.

33. Marguerie A, Bajolle F, Zaffran S, Brown NA, Dickson C, Buckingham ME, et al. Congenital heart defects in Fgfr2-IIIb and Fgf10 mutant mice. Cardiovasc Res. 2006;71(1):50-60.

34. Park EJ, Watanabe Y, Smyth G, Miyagawa-Tomita S, Meyers E, Klingensmith J, et al. An FGF autocrine loop initiated in second heart field mesoderm regulates morphogenesis at the arterial pole of the heart. Development. 2008;135(21):3599-610.